The Cryosphere Discuss., 5, 131–167, 2011
www.the-cryosphere-discuss.net/5/131/2011/
doi:10.5194/tcd-5-131-2011

The Cryosphere Discussions

Variability and changes of Arctic sea ice thickness distribution under different AO/DA states

A. Oikkonen[1] **and J. Haapala**[2]

[1]Univ. of Helsinki, Department of Physics, P.O. Box 48, 00014 University of Helsinki, Finland
[2]Finnish Meteorological Institute, Helsinki, Finland

Received: 21 December 2010 – Accepted: 21 December 2010 – Published: 12 January 2011

Correspondence to: A. Oikkonen (annu.oikkonen@helsinki.fi)

Published by Copernicus Publications on behalf of the European Geosciences Union.

Abstract

Changes of the mean sea ice thickness and concentration in the Arctic are well known. However, comparable little is known about the ice thickness distribution and the composition of ice pack in quantity. In this paper we determine the ice thickness distributions, mean and modal thicknesses, and their regional and seasonal variability in the Arctic under different large scale atmospheric circulation modes. We compare characteristics of the Arctic ice pack during the periods 1975–1987 and 1988–2000, which have a different distribution in the AO/DA space. The study is based on submarine measurements of sea ice draft.

The prevalent feature is that the peak of sea ice thickness distributions has generally taken a narrower form and shifted toward thinner ice. Also, both mean and modal ice thickness have generally decreased. These noticeable changes result from a loss of thick, mostly deformed, ice. In the spring the loss of the volume of ice thicker than 5 m exceeds 35% in all regions except the Nansen Basin, and the reduction is as much as over 45% at the North Pole and in the Eastern Arctic. In the autumn the volume of thick, mostly deformed ice has decreased by more than 40% in the Canada Basin only, but the reduction is more than 30% also in the Beaufort Sea and in the Chukchi Sea. In the Beaufort Sea region the decrease of the modal draft has been so strong that the peak has shifted from multiyear ice to first-year type ice. Also, the regional and seasonal variability of the sea ice thickness has decreased, since the thinning has been the most pronounced in the regions with the thickest pack ice (the Western Arctic), and during the spring (0.6–0.8 m per decade).

1 Introduction

The Arctic Ocean is known to exhibit a large climate variability. On a time scale of decades, the variability is largely driven by the large-scale atmospheric circulation, which alters meridional heat and moisture transport from the mid-latitudes to the Arctic

TCD
5, 131–167, 2011

region and, as a consequence, alters the surface heat balance of the Arctic Ocean. Another, perhaps more significant, effect is that sea ice and ocean surface circulation patterns are modified in accordance with the atmospheric changes.

The state of the atmospheric circulation is commonly described by the empirical orthogonal function (EOF) of the surface air pressure field. The first EOF is called the Arctic Oscillation (AO) or Northern Annular Mode (Thompson and Wallace, 1998). This mode is related to the magnitude of the zonal circulation (Rigor et al., 2002; Zhang et al., 2000). The second mode is called the Dipole Anomaly (DA) (Wu et al., 2006; Watanabe et al., 2006). DA is a measure of the strength of an atmospheric meridional circulation from the Pacific sector to the North Atlantic. Wu et al. (2006) state that the influence of the DA on winter sea ice motion is greater than that of the AO, especially in the Central Arctic basin, and north of the Fram Strait. During its positive phase DA has a particularly strong effect on the ice conditions, since in addition to the strengthening of the Transpolar Drift, and export of sea ice from the Arctic Ocean to Fram Strait, it also enhances an inflow of Pacific water into the Arctic.

Recently, many papers have focused on sea ice changes and the relationship between the atmospheric circulation and sea ice conditions (e.g., Hilmer and Lemke, 2000; Zhang et al., 2000; Holloway and Sou, 2002; Makshtas et al., 2003; Bitz and Roe, 2004; Rothrock and Zhang, 2005; Kwok, 2009), but previous analyses have been limited to considering mean sea ice thickness, concentration, or drift. However, the state of the ice pack is best characterized by the sea ice thickness distribution, defined as follows

$$\int_{h_1}^{h_2} g(h)dh = \frac{1}{R}A(h_1,h_2)\,, \qquad (1)$$

where R denotes the total area of the region, and $A(h_1,h_2)$ is the area within region R covered by ice with thickness h in the range $h_1 \le h < h_2$ (Thorndike et al., 1975). The ice thickness distribution $g(h)$ has dimension L^{-1}, but the distribution can be presented as

TCD
5, 131–167, 2011

a dimensionless fraction if $g(h)$ is multiplied by the bin width of the distribution dh.

Pack ice can be understood as being composed of three main ice types: first year ice (FYI), multi-year ice (MYI), and deformed ice. Ice types cannot be separated unambiguosly within an observed ice thickness distribution, since their thicknesses overlap. However, certain ice thickness categories are dominated by a particular ice type. FYI has experienced no more than one growth and one melting season, and on the basis of the model of Maykut and Untersteiner (1971) it can be assumed to reach a maximum of about 2 m at the end of the growth season, and about 1 meter in the autumn after the summer melt, which gives the upper limits for FYI thickness during the seasons of annual maximum and minimum thicknesses. In the sea ice thickness distribution $g(h)$, ice thicker than FYI consists of MYI and deformed ice. The thickness of level MYI approaches the equilibrium thickness, which can be set as the upper limit for MYI, i.e., 3–5 m depending on climatological conditions. Ice thicker than the equilibrium thickness is mostly deformed.

The typical shape of $g(h)$ depends on the climatological conditions. In the perennial ice zone (PIZ) sea ice is present during all seasons, while in the seasonal ice zone (SIZ) the ocean is ice-free by the end of the summer. Ice thickness distributions in PIZ and SIZ have distinct characteristics that vary seasonally. In the spring, both in PIZ and in SIZ, $g(h)$ typically has one clear peak at a location typical for FYI in SIZ and for MYI in PIZ. In the autumn, PIZ typically has a bi-modal thickness distribution with the modal thickness in MYI, a second maximum in very thin FYI, and a local minimum between these. In SIZ in the autumn, $g(h)$ is dominated by very thin FYI and open water, and thicker ice types have relatevely small concentrations.

The evolution of $g(h)$ depends on the thermodynamic and dynamic forcing factors. Changes in those factors have different impacts on the shape of $g(h)$, and in some situations an evaluation of changes in $g(h)$ reveals whether the observed changes in the pack ice are due to predominantly thermodynamic or dynamic processes.

Thermodynamic effects change the position of the modal peaks of FYI and MYI. Kurtosis, i.e., the shape of the modal peak of $g(h)$, is a measure of the relative contribution

TCD
5, 131–167, 2011

A. Oikkonen and J. Haapala

of dynamic effects. Pure thermodynamic forcing (the case of fast ice) would result in a single-peak distribution. The effect of the dynamics (opening, redistribution, and advection of pack ice) widens the single-peak distribution. On a regional scale, changes in the circulation and influx of sea ice could result in large changes in $g(h)$. Shifts in differential ice drift have an effect on both ends of $g(h)$. Changes in lead opening are reflected in the fraction of open water and thin ice, and changes in ridging are seen in the tail of $g(h)$.

However, sea ice thermodynamic and dynamic processes are strongly coupled, and in some situations it is difficult to separate these effects. For example, the longer the ice circulates in the Arctic, the more time it has to grow both thermodynamically and through deformations. Thus, the change in the drift pattern and average travel time can cause significant changes both in the modal thickness and in the fraction of ridged ice.

Our approach is to compare ice thickness distributions during two periods dominated by different large-scale atmospheric circulation. We utilize data from submarine cruises of the US Navy and the Royal Navy (NSIDC) from the years 1975–2000. The 26 years covered by the available data are divided into two periods, 1975–1987 and 1988–2000. Although the division is somewhat arbitrary, it coincides with changes in climatologic and oceanographic conditions in the Arctic, e.g., a decrease of sea level pressure (SLP) in the Central Arctic at the end of the 1980s (Walsh et al., 1996), and a change in the AO index from a mostly negative to a strongly positive phase in 1988 (Rigor et al., 2002).

As Wang et al. (2009) showed, the major atmospheric circulation patterns of the Arctic are well described by the modes of AO and DA. In general, when AO and DA are positive, the atmospheric circulation strengthens the transpolar drift, and enhances export of sea ice from the high Arctic to the Fram Strait. Figure 1 depicts how the individual years of the two periods examined in this paper are placed in an AO/DA space. It is clear that the period 1975–1987 was dominated by negative AO and DA years: average AO and DA values were -0.17 and -0.24, respectively. The later period also includes negative AO and DA years, between 1996–2000, but positive AO

TCD
5, 131–167, 2011

and DA years prevailed at the beginning of the period. Also, the most anomalous years as regards DA occurred during the later period.

The objective of the present paper is to examine changes of the sea ice thickness distribution in detail. The submarine dataset has previously been analyzed by Wensnahan and Rothrock (2005), Rothrock and Wensnahan (2007), and Belchansky et al. (2008). Those papers focus on the quality of the dataset, and changes in the mean sea ice thickness in the Arctic Ocean. The goal of this paper is to determine the changes and variability of the Arctic sea ice thickness distribution on a regional scale. The analysis is conducted for the spring and the autumn, i.e., for the periods of annual maximum and minimun ice thickness. Particular attention is given to the analysis of changes in the composition of pack ice, and to the evaluation of the impact of thermodynamics and dynamics on the evolution of the Arctic sea ice cover.

2 Data and analysis

The US Navy and Royal Navy upward-looking sonar data set includes sea ice draft measurements from 37 cruises accomplished during the years 1975–2000, covering over 120 000 km of track in total. Data are archived for public use at the US National Snow and Ice Data Center (NSIDC). Data has been recorded partly in analog, and partly in digital format. The error in the comparability of analog data with digitally recorded data is ±6 cm (Wensnahan and Rothrock, 2005), which is very small compared with draft values of typically several meters, and in this study data collected in both formats have been used. The standard deviation of submarine sonar measurements is 25 cm, and the draft measurements are biased by +29 cm compared with the true draft (Rothrock and Wensnahan, 2007).

This study concentrates on the spring (April and May) and the autumn (September and October), because this gives the best sampling density, and the possibility to study the behavior of annual maximum and minimum thicknesses (Rothrock et al., 1999). From here on, Spring refers to April and May, and Autumn refers to September and

TCD
5, 131–167, 2011

October. The cruises were equally distributed within each season during the whole study period, and no temporal adjustment is made for the date of the measurements.

The 26 years covered by the available data are divided into two periods, 1975–1987 and 1988–2000. In total, the former half includes data from 12 cruises, of which 9 were accomplished in Spring and 3 in Autumn, while the later half includes data from 11 Spring cruises and 8 Autumn cruises. To study the regional variability and possible changes in this, the area of the data is divided into six regions as shown in Fig. 2.

Analyses are made using profile data that include all measurements with an interval of about one meter. Regional mean drafts and draft distributions are calculated from all the point measurements recorded within one region during the period and season concerned. The number of measurements used in each region, season, and period is listed in Table 1. In total the number of recordings utilized is over 78 000 000, corresponding to roughly 78 000 km of submarine track.

Mean draft values also include recordings of open water. All analyses are made, and the results are presented, using the values of draft instead of thickness, because an accurate conversion from draft to thickness would require knowledge of the density of sea ice, as well as the thickness and the density of the snow cover. The variability and changes of the Arctic sea ice cover are also examined through the evolution of three ice categories, classified by draft (D). Category 1 includes all the ice with D<2 m in Spring and D<1 m in Autumn. Hence, this category consists mainly of FYI. Category 2 is dominated by MYI, and the upper limit is set at D=5 m. Category 3 consists of ice with draft D>5 m, and this category is dominated by deformed ice (Wadhams and Davis, 2001).

3 Results

Our approach is to look at the changes and variability of the Arctic ice pack on a regional scale during two seasons, Spring and Autumn. Throughout this section results are presented for each of the six regions (Fig. 2), separately for Spring and Autumn,

TCD
5, 131–167, 2011

and for two periods of 13 years, 1975–1987 and 1988–2000. First we look at regional ice draft distributions, and modal and mean drafts. Later, changes in the ice pack are described also by looking at regional ice volume distributions, and by examining the contribution of different ice categories to the total ice volume.

3.1 Ice draft distribution

Probability density functions of ice draft, i.e., draft distributions $g(D)$ are calculated with an interval of 20 cm for each region, for both of the 13-year periods 1975–1987 and 1988–2000, and separately for Spring and Autumn (Figs. 3 and 4). Corresponding modal drafts are listed in Table 2. All regional Spring draft distributions from the first period (Fig. 3, solid line) have quite a uniform shape with one wide peak at draft 2–3 m, which falls into ice category 2, and into the typical range of MYI. Regional differences are most pronounced in the fraction of open water and thin ice, $D<0.5$ m. Compared to the first period, Spring draft distributions from 1988–2000 (Fig. 3, dashed line) have much higher and narrower peaks, located in thinner ice, $D=1.5$–2.5 m, and their regional variability is larger. In regions 1, 2, 5 and 6, i.e., in the Central and Eastern Arctic, Spring draft distributions show clear narrowing and heightening of the peak, due to a noticeable increase of ice with a draft of 1–3 m and a decrease of other thicknesses. In regions 1 and 2 (the North Pole and the Canada Basin) modal draft in Spring is in MYI-dominated category 2 during both periods, despite a modest decrease (−0.4 m and −0.2 m, respectively, Table 2). In region 5 (Eastern Arctic) Spring modal draft has decreased from 2.5 m to 2.1 m, but the shape of the peak has changed noticeably to a narrower and higher form. This is caused by a strong increase of ice with a draft of 1–3 m, and a clear decrease of ice with $D>3$ m. In the Western Arctic, in regions 3 and 4, the modal draft in Spring has decreased from 2.5 m to 1.7 m, and from 2.5 m to 1.5 m, respectively. In these regions the peak has shifted from ice category 2 to category 1, i.e., from the dominance of MYI to the draft range of FYI.

Autumn draft distributions from 1975–1987 (Fig. 4, solid line) differ clearly from Spring cases. The shape of Autumn draft distributions has a large regional variability.

TCD
5, 131–167, 2011

However, all the distributions, except region 4 (the Chukchi Sea), have a local minimum around D=0.5–1 m, on the boundary between FYI and MYI. Draft distributions from 1988–2000 (Fig. 4, dashed line) show that a bi-modal structure has become stronger in the Central Arctic (regions 1 and 2) as the concentration of thin FYI has increased, and the concentration of thick, mostly deformed ice has decreased. Concentration of very thin ice (D<0.4 m) has roughly doubled around the North Pole (region 1), and tripled in region 2 (the Canada Basin), resulting in a clear second maximum at D=0.3 m. Also ice with D=1.5–2.5 m (mostly thin MYI) has increased in these two regions, while thicker ice has decreased. In Autumn the modal draft has remained unchanged in the Eastern Arctic (region 5). However, the shape of the draft distribution has changed from one high peak to a clearly bi-modal structure, as the fraction of open water and thin ice with D<0.4 m has more than doubled, and the fraction of ice around D=2 m (mainly MYI) has decreased by nearly 40%. The Autumn draft distribution in region 6 has remained almost unchanged. In general, changes in the modal draft are smaller in Autumn than in Spring, and region 3 (the Beaufort Sea) is the only region showing a strong decrease (−1.0 m) while in regions 2 and 4 (the Canada basin and the Chukchi Sea) the modal draft has increased by 0.2 m (Table 2).

Draft distributions can be divided into two groups with the characteristics of PIZ and SIZ. In PIZ the Autumn draft distribution typically has a bi-modal shape, with a modal draft in MYI and a second maximum in FYI. This is the case in regions 1, 2, 5 and 6 (the North Pole, the Canada Basin, the Eastern Arctic and the Nansen Basin) during both periods, and in region 3 (the Beaufort Sea) during the first period. In these regions the modal draft is around 2–3 m, the second maximum is in thin FYI (D=0.3 m), and there is a local minimum between them at D=0.7–0.9 m. In SIZ the Autumn draft distribution is dominated by open water and thin FYI, which is the case in region 4 (the Chukchi Sea) during both periods and in region 3 (the Beaufort Sea) during the later period. In these regions the draft distributions do not show any clear boundary between FYI and MYI, since the distribution is high and fairly even for drafts 0.5–2 m, but the concentration of ice thicker than D=2 m decreases rapidly with increasing draft.

TCD
5, 131–167, 2011

In region 3 (the Beaufort Sea), the ice cover has clearly changed from perennial to seasonal. The height and width of the peak in the Spring draft distribution have remained the same, but the location has shifted to much thinner ice, from ice category 2 to category 1 (MYI to FYI). In Autumn, the change is most pronounced in thin ice ($D<0.6$ m), which has increased so much that a local minimum around 0.5 m, present in 1975–1987, has disappeared. During the first period the shape of the Autumn draft distribution in region 3 has the characteristics of PIZ, showing a bi-modal shape with peaks in FYI and MYI, and clear minimum between them, in contrast to the later period, when the shape of the Autumn draft distribution is very representative of SIZ.

The regional Spring and Autumn mean drafts for the periods 1975–1987 and 1988–2000 are presented in Table 2. In Spring, in regions 3 and 5 (the Beaufort Sea and the Eastern Arctic) the mean draft has noticeably decreased, by about 1 m. In regions 1, 2 and 4 (the North Pole, the Canada Basin, and the Chukchi Sea) the Spring mean draft also has clearly decreased, by 0.7 m or more. In Autumn, changes in general are more modest, and region 2 (the Canada Basin) is the only region where the decline in the Autumn mean draft exceeds the thinning in Spring. In regions 1, 3 and 5, the decrease of the Autumn mean draft is only about 30% of the decrease observed in Spring. In region 4 the Autumn mean draft has increased by 0.2 m. In region 6 (the Nansen Basin) the mean draft has remained nearly unchanged in both Spring and Autumn, and actually shows a slight increase of about 0.1 m. However, in view of the accuracy of the draft measurements, changes with a magnitude of 0.1 m cannot be regarded as significant.

3.2 Ice volume

The probability density function of ice volume is calculated after Yu et al. (2004), but as a function of draft D, $V(D)=g(D)D$. This function is dimensionless and describes the fraction of total volume of ice with draft D. It integrates to the mean draft (Yu et al., 2004)

TCD
5, 131–167, 2011

$$\overline{D} = \int_0^\infty V(D)dD\,. \quad (2)$$

Because they are defined using draft instead of thickness, the volumes presented here correspond to the portion of the total ice volume that is under the water level. As Eq. (2) shows, the total ice volume per unit area equals the mean draft, but the benefit of this approach as compared with calculating the mean draft by directly averaging single measurements is that it makes it possible to determine the composition of the total ice volume.

Cumulative ice volume distributions from the periods 1975–1987 and 1988–2000 in all the regions are shown in Fig. 5, separately for Spring and Autumn. Percentual changes in the total Spring and Autumn ice volumes are listed in Table 3. The total ice volume is here determined as the sum of the volumes in each bin, i.e., the cumulative volume in the thickest ice bin.

Region 6 is the only area where the total ice volume has remained nearly unchanged in both seasons; it even shows a very slight increase. In all other regions the total Spring ice volume has decreased by over 15%, which is caused by the loss of thick ice. The reduction of the total Spring ice volume is largest in region 3 (the Beaufort Sea), where the decline is nearly 30% due to a considerable reduction of ice with $D>3$ m. At the same time, the volume of FYI ($D<2$ m) is nearly twice as large during the later period. In region 4 (the Chukchi Sea), the evolution of the Spring ice volume is very similar to region 3 (the Beaufort Sea), but in regions 1 and 2 (the North Pole and the Canada Basin) the decline is more modest (–18% and –17%, respectively) and the volume loss has occurred in thicker, mostly deformed ice (in $D>8$ m and $D>5$ m, respectively).

In Autumn the change in the total ice volume is largest in region 2 (–24%), which is the only region where the decline is greater in Autumn than in Spring. Evolution of the Autumn ice volume is exceptional in region 4, where the total Autumn ice volume has

TCD
5, 131–167, 2011

increased by 19%, and the increase is pronounced in all ice categories with $D>1$ m.

3.3 Composition of the ice volume

As described above, there have been clear changes in the total ice volume in the whole study area, except in region 6 (the Nansen Basin). Also the composition of the total ice volume has changed, even in region 6. Figure 6 illustrates the composition of the regional Spring and Autumn total ice volumes of the three ice categories during both the 13-year periods. The percentual change in the volume of the three ice categories is listed in Table 3.

FYI has the dominant role in SIZ in Spring. As regional draft distributions show, region 4 (the Chukchi Sea) can be regarded as SIZ during the whole study period, and region 3 (the Beaufort Sea) has the attributes of SIZ during the later period. In addition to change in the ice draft distribution and corresponding changes in the concentration of different ice types, the change from a perennial to a seasonal type in region 3 is evident as seen in the remarkable increase of the volume of ice in category 1 (+176% in Spring and +45% in Autumn). Because of this large increase, during the later period about 25% of the total Spring ice volume consists of ice of the thinnest category, while during the former period the corresponding fraction is only 7%. The volume of ice of category 1 has increased also in PIZ, except in region 6 in Autumn, but even after the increase, this thinnest ice type comprises less than 10% of the total ice volume in PIZ.

The volume of MYI-dominated category 2 has generally decreased. The reduction has been strongest in region 3 (the Beaufort Sea) (−49% in Spring and −20% in Autumn) and in region 5 (the Eastern Arctic, −28% and −21%). In these regions the total volume of ice in categories 1 and 2 (roughly representing the volume of level ice) has decreased in both seasons despite the increasing volume of the thinnest ice type (mainly thin FYI). In Spring a similar evolution, though of smaller magnitude, can be seen also in region 4 (the Chukchi Sea). In region 1 (the North Pole) the volume of ice in category 2 in Spring has increased by more than 27%. Even though ice of category 2 can be assumed to be dominated by MYI, this increament does not necessarely

TCD
5, 131–167, 2011

mean an increase in MYI volume. It can, and most likely does, reflect a decrease in the thickness of deformed ice, with a greater proportion of thin deformed ice falling into ice category 2 ($D<5$ m). In Autumn region 4 (the Chukchi Sea) is the only region where a clear increase in the volume of ice in category 2 is observed. In region 6 (the Nansen Basin) changes are small, but in all other regions the volume of ice in category 2 in Autumn has decreased by about 10–20%.

Ice in category 3 consists mostly of deformed ice. Evolution of this ice category is regionally and seasonally the most uniform of all the observed changes. As draft distributions show, the concentration of deformed ice has decreased in all regions both in Spring and in Autumn. Since the thickest ice types have a great deal of weight in the total ice volume, the decrease in the concentration of deformed ice is largely responsible for the reduction in the total ice volume that is observed in almost all the regions. In general, the volume of the thickest ice, which is mostly deformed, has decreased more strongly in Spring than in Autumn, and only in region 2 does Autumn show a greater decrease than Spring. In Spring the loss of category 3 ice volume exceeds 35% in all regions except region 6, and the reduction reaches over 45% in regions 1 and 5 (the North Pole and the Eastern Arctic). In Autumn the volume of ice in category 3 has decreased by more than 40% in region 2 (the Canada Basin) only, but the reduction is more than 30% also in regions 3 and 4 (the Beaufort Sea and the Chukchi Sea). In region 6 (the Nansen Basin) changes have been considerably smaller than in all other regions, −7% in Spring and no change in Autumn.

Figure 6 as well as Fig. 5 confirm that the loss of thick, deformed ice is largely responsible for the decline in the total ice volume. This is most evident during Spring in regions 1 and 2 (the North Pole and the Canada Basin), where the volume of ice categories 1 and 2 (roughly corresponding to level ice) has even increased, and thus the reduction in total ice volume of over 17% has occurred purely due to the loss in the thickest ice category, i.e., deformed ice. In regions 3, 4 and 5 the volume of ice category 2 has also decreased in Spring, but not as strongly as the volume of category 3, and as the result of these changes the total ice volume has decreased by more than

TCD
5, 131–167, 2011

20%. If the loss of deformed ice volume is not due to a decrease in the number of ice ridges only, but also due to a decreasing ridge thickness, then more deformed ice may fall into ice category 2. In that case, the reduction of MYI volume may be larger than the decrease of category 2 ice volume directly shows.

4 Discussion

4.1 Thinning rate

Regional mean drafts (Table 2) show considerable decrease in most of the regions, but with large regional and seasonal differences. Thinning of the Arctic sea ice cover has been observed in several studies (e.g., Wadhams, 1990; Rothrock et al., 1999; Wadhams and Davis, 2000; Tucker et al., 2001; Yu et al., 2004). These studies are based on submarine sonar measurements, but from different years and seasons as well as from different areas, so that comparison of results is not straightforward. Overall, in all the previous studies, as well as in our work, the observed thinning follows a similar regional pattern, with the largest changes in the Central and Western Arctic. These are the regions that are most often included in the study area, and where the sampling is most complete. In other regions, results of different studies covering different seasons and different periods have much more variation, and results are based on more sparse sampling.

Rothrock et al. (1999) and Yu et al. (2004) compared Autumn mean drafts from four historical submarine cruises (from late 1950s to 1970s) with three more recent ones (1993–1997). They both reported strong thinning in the Central and Western Arctic, i.e., in the North Pole region, the Canada Basin and the Beaufort Sea, with a rate of approximately -0.4 m per decade. This is about double the Autumn thinning rate in the North Pole region and the Beaufort Sea (regions 1 and 3) that we present in Table 2, but slightly less than that observed in the Canada Basin (region 2). Rothrock et al. (1999) reported strong thinning also in the Chukchi Sea, while Yu et al. (2004) did not find any significant change in this region. Both of these findings differ from the changes found in the present study, since for the period 1975–2000 the Chukchi Sea (region 4) shows an increase in Autumn mean draft with a rate of +0.2 m per decade. In the Eastern Arctic the thinning rates observed by Rothrock et al. (1999) and Yu et al. (2004) differ clearly from each other (−0.6 and −0.1 m per decade, respectively), and the rate observed in the present study (−0.3 m per decade) lies between them. Comparison of the years 1958–1970 and 1993–1997 in Rothrock et al. (1999) showed that the Nansen Basin, together with the Eastern Arctic, is the region of strongest thinning, while the present study covering the years 1975–2000 does not show any significant change in the region.

On the other hand, Wadhams (1990) and Wadhams and Davis (2000) observed strong thinning in the Nansen Basin also between the years 1976 and 1996. These works are based on the data that is not included in the public archive of NSIDC, and the cruise tracks extended further south than any of the Autumn cruises utilized in the present study. Wadhams and Davis (2000) observed the strongest thinning rates in the southernmost part, between latitudes 81° N–83° N, where the mean draft in 1996 was only about 30% of the mean in 1976. In any case, also in the latitudes better covered by the data of NSIDC Wadhams and Davis (2000) reported thinning rates clearly larger than those presented here. The explanation for the strong difference is probably due to the spatial and temporal averaging method. Wadhams and Davis (2000) compared data from two cruises in a very narrow sector, while in the present study comparison is made over a larger area and between two 13-year periods. On the basis of earlier observations of thinning in the same region (Wadhams, 1990), Wadhams and Davis (2000) concluded that a substantial part of the thinning took place before 1986, in a period that is not very well covered in the Autumn data set of NSIDC.

Tucker et al. (2001) has also examined changes in the mean draft on the basis of submarine sonar data, but in contrast to Rothrock et al. (1999), Yu et al. (2004), Wadhams (1990) and Wadhams and Davis (2000) they used data from Spring cruises. For the period 1986–1994 Tucker et al. (2001) observed very strong thinning in the Western

Arctic (about -1 m decade^{-1}) but the change in the North Pole region was insignificant. The longer time period considered in our analyses reveals smaller thinning rates in the Beaufort Sea and the Canada Basin (-0.8 and -0.6 m per decade, respectively), but in the North Pole region the situation is the opposite, and the longer time period shows much stronger thinning (-0.6 m per decade) than reported by Tucker et al. (2001).

The strongest thinning in the Western and Central Arctic, which are the regions of initially the thickest ice, has led to a decline in regional variability, and to a more uniform distribution of sea ice mass over the Arctic Ocean. A similar spatial pattern has also been observed in several model studies (e.g., Zhang et al., 2000; Bitz and Roe, 2004). In addition to the regional variation, the thinning rates presented in Table 2 have also considerable seasonal differences. The thinning has generally been larger in Spring than in Autumn, which means a decrease in seasonal variability. Earlier analyses of submarine sonar measurements have focused on one season only, and therefore they have excluded the seasonal aspect of the thinning rate. Changes in the seasonal variability have not been much discussed in model studies, either. Hilmer and Lemke (2000) estimated the annual cycle of thinning based on dynamic-thermodynamic sea ice modelling, and found the largest decrease in the mean thickness in Autumn, contrary to the results based on observation presented here.

4.2 Composition of the ice cover

As described above, the thinning rates estimated in different studies vary considerably, even though many of them are based partly on the same data. In any case, all these studies are in very good agreement as regards the changes in the composition of ice volume, consistent with the results presented in this paper. E.g. Wadhams and Davis (2001), Tucker et al. (2001) and Yu et al. (2004) reported a clear decrease in the concentration and fractional volume of thick, mostly deformed ice. In the present study also, the strongest as well as the seasonally and regionally most uniform of all observed changes is the loss of thick ice, which is evident in draft distributions (Figs. 3–

TCD
5, 131–167, 2011

A. Oikkonen and J. Haapala

Title Page
Abstract | Introduction
Conclusions | References
Tables | Figures
◂◂ | ▸▸
◂ | ▸
Back | Close
Full Screen / Esc
Printer-friendly Version
Interactive Discussion

4), and even more clearly visible in the cumulative ice volume distributions (Fig. 5). From Fig. 5 it is evident that the decline in ice volume occurred due to the loss of thick ice, with some regional variance in the limiting draft.

Tucker et al. (2001) reported that in the Canada Basin (at 86° N) the occurrence of deformed ice, which they defined as $D>3.5$ m, was about 20% smaller in the 1990s than in the 1980s. In the North Pole region, Tucker et al. (2001) did not find changes that strong, even though the concentration of FYI showed a slight increase, and the concentration of deformed ice showed a small decrease. Our analyses cover a longer time period and a larger area. In the Canada Basin our results are in very good agreement with Tucker et al. (2001). However, in the North Pole region the longer time period presented here reveals much larger changes than reported by Tucker et al. (2001).

The observation of a significant change in the Beaufort Sea from PIZ type to SIZ type is supported by e.g., Comiso (2002). They observed significant year-to-year variation in the location of PIZ, depending mostly on ice drift forced by atmospheric circulation, but also a clear reduction in the extent of PIZ during 1978–2000. The change was strongest in the Beaufort Sea and the Chukchi Sea, and considerable changes took place also in the eastern part of the Arctic Ocean (Comiso, 2002).

Changes in the extent of Arctic sea ice, and especially in the extent of PIZ, have continued and even accelerated since 2000 (e.g., Maslanik et al., 2007; Comiso et al., 2008). Maslanik et al. (2007) point out that in addition to the retreat of PIZ as a whole, the amount of oldest and thickest ice within the remaining MYI pack has decreased significantly. In the mid-1980s 35% of MYI consisted of ice about 2–3 years old, but by 2007 the corresponding fraction had increased up to nearly 60% (Maslanik et al., 2007). The decrease of the modal draft up to the year 2000 (Table 2), as well as the reduction of the volume of ice in category 2 (Table 3) reflects a similar change in the average age of the ice. Even though the ice category 2 can be assumed to be dominated by MYI, changes in the ice volume in this category do not necessarily directly show a change of MYI volume. The thickness ranges of MYI and deformed ice are partly overlapping, and in the case of decreasing average ice ridge thickness, more and more deformed ice may fall into the ice category 2. Thus, thinner deformed ice may partly compensate the loss of MYI in ice category 2 and lead to an underestimate of the decrease in MYI volume.

4.3 Thermodynamic forcing

The thermodynamical growth and decay are determined by energy balances at the atmosphere-ice and ice-ocean interface. Although the observed loss of ice volume is due to the strong reduction of thick, mostly deformed ice, it could be caused by changes in the thermodynamical forcing by several possible mechanisms. First, thinner, thermodynamically grown, undeformed sea ice presumably forms thinner sea ice ridges in deformations. On the other hand, it is possible that the decreasing effect on mean thickness and ice volume would be seen only on the scale of individual ridges, and the effect on a regional scale would be the opposite, since thinner ice is more easily deformed, and the number of ridges would increase. Second, the increase of the oceanic heat flux enhances bottom melting with the strongest effect on ice ridges, due to their larger surface area and the turbulence caused by keels (Yu et al., 2004). An increase in the oceanic heat flux can be a result of a thinner and more open ice cover, which increases the absorption of solar radiation into the ocean. Also the retreat of the insulating cold halocline layer in the Eurasian Basin at the beginning of the 1990s has probably increased the oceanic heat flux, at least for some of the time, and the effect may have been enhanced by increased storm activity (Steele and Boyd, 1998). The increase in the temperature of the Pacific water entering through the Bering Strait has increased the oceanic heat flux in the Pacific sector of the Arctic also (Shimada et al., 2006). During the positive phase of DA the inflowing volume of Pacific water to the Arctic Ocean is also enhanced (Wu et al., 2006).

The surface air temperature (SAT) in the Arctic shows a positive trend, with the greatest rate in the winter and spring, and on the eastern side of the Arctic (e.g., Rigor et al., 2000; Polyakov et al., 2003). On the other hand, in the Beaufort Sea and the Canadian Archipelago winter time SAT shows nearly equally strong cooling (Rigor et al., 2000).

TCD
5, 131–167, 2011

However, the length of the melt season seems to be increasing in the entire Arctic Ocean, including also these western parts (Belchansky et al., 2004). Belchansky et al. (2004) found a connection between the AO index and the length of the melt season. Following winters with a high AO index the melt season tends to be longer, due to both an earlier melt in the spring and a later freeze in the autumn. Belchansky et al. (2004) observed a very strong lengthening of the melt season, up to 2–3 weeks, beginning in the year 1989, concurrent with a strong increase in the winter AO index. This shift took place at the beginning of the second period used in our analyses (1988–2000), and thus conditions during this later period have favored more melting and less ice growth.

Even though Zhang et al. (2000) concluded that the interannual changes in the Arctic ice volume are primarily forced by ice dynamics, they also state that changes in lateral melting from thermodynamic forcing are much more important than changes in ice growth. Their model results showed a decrease in net ice production in the whole Arctic, which was entirely due to an increase in lateral melting. However, changes in lateral melting are closely related to changes in ice advection and surface albedo, and the result of a complex interplay between dynamics and thermodynamics.

How do the observed changes in ice thickness distributions during 1975–2000 (Figs. 3 and 4) reflect the changes in the thermodynamics? The kurtosis of ice thickness distributions, especially in Spring (Fig. 3) has generally increased, and the peaks have also shifted towards thinner ice. The narrowing of the peak may reflect the increasing impact of thermodynamic forcing, and the shift of the peak may indicate the change in this forcing factor, now towards less ice growth and/or more ice melt. On a regional scale, however, changes in circulation and ice advection can cause significant changes that are at least partly similar. As described above, the dominance of thermodynamics could explain the decrease of the modal thickness of MYI, and also the observed loss of thick, deformed ice, but the warming trend in SAT, the lengthening of the melt season, and the increase in the oceanic heat flux do not offer a comprehensive and straightforward explanation for the decrease in the seasonal and regional variability. At the same time, it must be taken into account that, as Bitz and Roe (2004)

Discussion Paper | Discussion Paper | Discussion Paper | Discussion Paper |

TCD

5, 131–167, 2011

Variability and changes of Arctic sea ice

A. Oikkonen and J. Haapala

showed, the response of ice to the changing SAT depends on the initial thickness, and thus a small increase of SAT in the areas, and during the seasons, of thickest ice can cause a large decline in thickness.

4.4 Dynamic forcing

Several studies have concluded that dynamical forcing has had a dominant role in the strong thinning of the Arctic sea ice cover. Makshtas et al. (2003) state that only 20% of the thinning can be explained by an increase in SAT, and most of the reduction is caused by a decrease in ridge concentration. Other approaches to the question can be found in e.g., Rigor and Wallace (2004), who point out the decrease in the age of ice due to changes in the advection, and e.g., Vinje (2001) who associate the increase in ice export with the decreasing ice thickness in the Arctic.

The clear shift in the AO index from a mostly negative to a strongly positive phase in the late 1980s caused the weakening of the anticyclone around the Beaufort Sea (Rigor et al., 2002). According to Zhang et al. (2000) it can be assumed that the changes in the strength of Beaufort Gyre have the largest effect on ice conditions in the Eastern Arctic, causing a strong decrease in ice volume there, accompanied by a modest increase in ice volume in the Western Arctic.

In addition to the AO index, variations of the DA index also have an effect on ice drift patterns, and Wu et al. (2006) state that the influence of the DA on winter sea ice motion is greater than that of the AO, especially in the Central Arctic basin and north of Fram Strait. The positive phase of the DA includes a weakening of the Beaufort Gyre and a strengthening of the Transpolar Drift, which means an increase in ice export through Fram Strait and enhanced ice import from the Laptev and East Siberian Seas to the Central Arctic (Wu et al., 2006). The DA displays a strong interannual variability, but it does not show any apparent trend. In any case, the time series of the DA shows several years of very high values from the late 1980s to the late 1990s (Wu et al., 2006).

TCD
5, 131–167, 2011

Watanabe et al. (2006) studied the effect of different combinations AO and DA indexes by defining four states: positive AO and positive DA (state 1), positive AO and negative DA (state 2), negative AO and positive DA (state 3), negative AO and negative DA (state 4). Figure 1 shows annual values of AO and DA indexes during the periods 1975–1987 and 1988–2000, and how these years are located in the four states of AO/DA. Watanabe et al. (2006) observed that the total sea ice export from the Arctic Ocean reaches a maximum in state 1, and a minimum in state 4. The record lows of summer sea ice extent have occurred in states 1 and 3 (Wang et al., 2009).

As Fig. 1 shows, our study periods 1975–1987 and 1988–2000 fall largely in different parts of the AO/DA space. During the first period more than half of the years fall in state 4, which is associated with very low ice export. During the later period the yearly values vary more, but most of the years are in state 1 or 2. A notable feature is that all the years of particularly high DA index values are in the later period (years 1988, 1995 and 1997) while very low DA index values are observed mostly in the first period. The AO index is more variable than DA, but as Watanabe et al. (2006) state, due to its strong meridionality DA seems to have a larger impact on the sea ice export than AO. This is supported by the variations in Arctic sea ice outflow through Fram Strait presented by Kwok (2009). The years of highest DA values (1988, 1995, 1997) show up as a peak in the outflow time series, and the years of very low DA values (1984, 1986 and 1991) correspond to low ice export.

Dynamic forcing seems to have been rather different during the two periods, 1975–1987 and 1988–2000. How is this reflected in the changes in ice thickness distributions, mean and modal thicknesses, and their regional and seasonal variability? For instance, very strong thinning in the Eastern Arctic (region 5) can be explained by the changes in ice circulation patterns resulting from a weakening of the Beaufort Gyre and a strengthening of the Transpolar Drift, driven by variations of the AO and DA indexes. In the later period, a larger proportion of the ice advected into this region comes from the Siberian coast, being thinner FYI. A region with a very different evolution, nearly unchanged ice conditions, is the Nansen Basin (region 6). There the influence of a change in the

TCD
5, 131–167, 2011

advection pattern is opposite, and it has balanced the effect of the increased SAT, the lengthening of the melt season, and the possible increase of the oceanic heat flux. During the former period ice entering the Nansen Basin is mostly from the SIZ of the Kara and Laptev Seas, while in the later period advection over the North Pole is stronger, and includes more thick ice from the Central Arctic and the Beaufort Gyre. In the Western Arctic, the weakening of the Beaufort Gyre changes the dynamical forcing, resulting in a decrease in both the average age of the ice and the level of compression.

Evolution of Autumn ice volume in the Chukchi Sea is exceptional compared with all the other regions: there the total ice volume has increased by about 20% due to the considerable increase in the volume of MYI-dominated ice category 2. The Chukchi Sea is part of the Beaufort Gyre, and therefore ice advection has an important role. The only reasonable explanation for the increase of the amount of MYI at the end of the melt season seems to be enhanced advection from the Western Arctic. This assumption agrees with the observed decline in the volume of ice category 2 in the Beaufort Sea and the Canada Basin.

4.5 Other contributors

A decline in seasonal variability is difficult to explain by changes in SAT, the oceanic heat flux, and ice dynamics. Other possible contributors could be e.g., precipitation, cloudiness, river discharges and oceanic current system. Actually all of these influence the thermodynamic growth, but their impact and importance are not as well known as the effect of SAT and the oceanic heat flux. Here, precipitation and cloudiness are discussed in more detail, since they could produce seasonally varying changes.

Polyakov et al. (1999) stated that in the regime dominated by cyclonic circulation in the Arctic Ocean, which was the case during most of the period 1988–2000, precipitation is increased in all seasons. Years of cyclonic circulation are in general warmer, but summer temperatures still remain at the melting point (Polyakov et al., 1999). Enhanced summer precipitation, if assumed to fall mostly in the form of snow, would increase the surface albedo during the melting season and thus retard melting, and,

TCD
5, 131–167, 2011

A. Oikkonen and J. Haapala

together with other processes, possibly lead to a decreased seasonal variability in ice thickness.

The cloud cover has a large effect on downwelling long wavelength radiation, and thus on thermodynamical ice growth, but cloudiness in the Arctic is rather poorly known, and global climate models show large differences in the simulated cloud cover over the Arctic. Eisenman et al. (2007) studied the equilibrium thickness of the Arctic sea ice with different longwave radiation due to a different cloud cover as produced by global climate models. They found the range of the equilibrium thickness to be 1–10 m with an intermodel range of $\pm 20\,\mathrm{W\,m^{-2}}$ in the downwelling longwave radiation. On the other hand, they also pointed out the importance of the surface albedo, since the tuning of the albedo by only ± 0.1 is sufficient to eliminate these large differences in equilibrium thickness caused by the range of downwelling longwave radiation.

The effect of cloudiness on the surface energy balance has a strong seasonal difference between summer and winter. Walsh and Chapman (1998) estimate that the difference in the net surface radiation between cloudy and clear sky conditions is strongly negative, over $-50\,\mathrm{W\,m^{-2}}$, in the summer and positive, about $20\text{–}30\,\mathrm{W\,m^{-2}}$, from September to March. The increased cloudiness would thus have a cooling effect during the summer, while in the winter the effect would be the opposite, and hence it could be a possible factor causing a decrease in the seasonal variability of ice thickness.

5 Conclusions

In this paper we determine changes in ice thickness distributions, mean and modal thicknesses, and their regional and seasonal variability, in the Arctic under different large scale atmospheric circulation modes. We have compared characteristics of the Arctic ice pack during the periods 1975–1987 and 1988–2000, which have different distributions in the AO/DA space (Fig. 1).

TCD
5, 131–167, 2011

A major finding of this study is that the shape of the sea ice thickness distribution has changed: the peak of the ice thickness distribution has generally narrowed and shifted toward thinner ice. A prevalent feature, apparent in all regions both in Spring and Autumn, is the loss of thick, mostly deformed ice, which is mainly responsible for the decrease in the mean and modal ice thicknesses. In Spring the loss of the volume of ice thicker than 5 m exceeds 35% in all regions except the Nansen Basin, and the reduction is as much as over 45% in the North Pole region and the Eastern Arctic. In Autumn the volume of thick, mostly deformed ice has decreased by over 40% only in the Canada Basin, but the reduction is more than 30% also in the Beaufort Sea and the Chukchi Sea. Results reveal also a decrease in the seasonal variability of the mean ice thickness, but with strong regional differences. The regional variability of the sea ice thickness has decreased, since the thinning has been most pronounced in the regions with initially the thickest ice cover.

Ice dynamics have an essential impact on ice thickness and its distribution over the Arctic Ocean. Changes in the dynamical forcing are evident in the studies of e.g., Rigor et al. (2002); Zhang et al. (2000); Wu et al. (2006); Kwok (2009), and they all show the strong connection between ice dynamics and AO, NAO, or DA. Our study periods 1975–1987 and 1988–2000 have different distributions in the AO/DA space. During the first period over half of the years fall in state 4, which is associated with very low ice export. During the later period most of the years are in states 1 or 2, and all the years of particularly high DA index values occur in the later period (the years 1988, 1995 and 1997).

The shift in the drift pattern, mostly due to the weakening of the Beaufort Gyre at the end of the 1980s, corresponds well with the observed strong thinning in the Beaufort Sea, the Canada Basin and the Eastern Arctic, and also with the unchanged thickness in the Nansen Basin. In the Western Arctic, thinning due to dynamical forcing results from the decrease in the average ice age, and in the level of compression, while in the Eastern Arctic thinning may have been caused by the shift in the origin of ice advection, leading to the dominance of SIZ on the Siberian coast. In the Nansen Basin, change

TCD
5, 131–167, 2011

in ice advection balanced the influence of the thermodynamics, as the origin of ice entering the region has shifted from the dominance of SIZ in the Kara Sea and the Laptev Sea to a dominance of PIZ around the North Pole.

Changes in the Arctic sea ice cover have continued and even accelerated during the last years, as shown by the extreme minima in ice extent recorded in September 2007 (Comiso et al., 2008). The changes in sea ice thickness characteristics described here, which occurred in the 1990s, have preconditioned the observed large decrease in the annual minimum sea ice extent. After the year 2000 there have been a few submarine cruises in the Arctic Ocean, but the data is not yet freely available. The data collected during these cruises will probably show even larger changes in the draft and volume distributions than presented in this study. Comparison of statistics from the 1990s with the recent measurements of sea ice thickness by an electromagnetic method (Haas et al., 2008, 2010) show that during the last years the peak of draft distributions has changed into an even narrower form, and shifted toward thinner ice in the North Pole region.

Acknowledgements. We want to acknowledge National Snow and Ice Data Center for providing submarine sonar data set. We also wish to thank Jia Wang for providing AO and DA time series. This study was funded through the EU FP7 project Damocles (Development Arctic Modelling and Observing Capabilities for Long-term environmental Studies). A. Oikkonen was also supported by Academy of Finland (project 11224121).

References

Belchansky, G. I., Douglas, D. C., Alpatsky, I. V., and Platonov, N. G.: Spatial and temporal multiyear sea ice distribution in the Arctic: a neural network analysis of SSM/I data, 1988–2001, J. Geophys. Res., 109, C10017, doi:10.1029/2004JC002388, 2004. 149

Belchansky, G. I., Douglas, D. C., and Platonov, N. G.: Fluctuating arctic sea ice thickness changes estimated by an in situ learned and empirically forced neural network model, J. Climate, 21, 716–729, doi:10.1175/2007JCL1787.1, 2008. 136

Bitz, C. M. and Roe, G. H.: A mechanism for the high rate of sea ice thinning in the Arctic Ocean, J. Climate, 17, 3623–3632, 2004. 133, 146, 149

Comiso, J. C.: A rapidly declining perennial sea ice cover in the Arctic, Geophys. Res. Lett., 29, 1956, doi:10.1029/20002GL015650, 2002. 147

Comiso, J. C., Parkinson, C. L., Gersten, R., and Stock, L.: Accelerated decline in the Arctic sea ice cover, Geophys. Res. Lett., 35, L01703, doi:10.1029/20007GL031972, 2008. 147, 155

Eisenman, I., Untersteiner, N., and Wettlaufer, J. S.: On the reliability of simulated Arctic sea ice in global climate models, Geophys. Res. Lett., 34, L10501, doi:10.1029/2007GL029914, 2007. 153

Haas, C., Pfaffling, A., Hendricks, S., Rabenstein, L., Etienne, J.-L., and Rigor, I.: Reduced ice thickness in Arctic Transpolar Drift favors rapid ice retreat, Geophys. Res. Lett., 1, L17501, doi:10.1029/2008GL034457, 2008. 155

Haas, C., Hendricks, S., Eicken, H., and Herber, A.: Synoptic airborne thickness surveys reveal state of Arctic sea ice cover, Geophys. Res. Lett., 37, L09501, doi:10.1029/2010GL042652, 2010. 155

Hilmer, M. and Lemke, P.: On the decrease of Arctic sea ice volume, Geophys. Res. Lett., 27, 3751–3754, 2000. 133, 146

Holloway, G. and Sou, T.: Has Arctic sea ice rapidly thinned?, J. Climate, 15, 1691–1701, 2002. 133

Kwok, R.: Outflow of Arctic Ocean sea ice into the Greenland and Barents Seas: 1979–2007, J. Climate, 22, 2438–2457, 2009. 133, 151, 154

Makshtas, A. P., Shoutilin, S. V., and Andreas, E. L.: Possible dynamic and thermal causes for the recent decrease in sea ice in the Arctic Basin, J. Geophys. Res., 108, 3232, doi:10.1029/2001JC000878, 2003. 133, 150

Maslanik, J. A., Fowler, C., Stroeve, J., Drobot, S., Zwally, J., Yi, D., and Emery, W.: A younger, thinner ice cover: increased potential for rapid, extensive sea-ice loss, Geophys. Res. Lett., 34, L24501, doi:10.1029/20007GL032043, 2007. 147

Maykut, G. A. and Untersteiner, N.: Some results from a time-dependent thermodynamic model of sea ice, J. Geophys. Res., 76, 1550–1575, 1971. 134

NSIDC: National Snow and Ice Data Center, Submarine upward looking sonar ice draft profile data and statistics, 1998, updated 2006. 136

Polyakov, I. V., Proshutinsky, A. Y., and Johnson, M. A.: Seasonal cycle in two regimes of Arctic climate, J. Geophys. Res., 104, 25761–25788, 1999. 152

Polyakov, I. V., Bekryaev, R. V., Alekseev, G. V., Bhatt, U. S., Colony, R. L., Johnson, M. A., Maskshtas, A. P., and Walsh, D.: Variability and trends of air temperature and pressure in the maritime Arctic, J. Climate, 15, 2067–2077, 2003. 148

Rigor, I. G. and Wallace, J. M.: Variations in the age of Arctic sea-ice and summer sea-ice extent, Geophys. Res. Lett., 31, L09401, doi:10.1029/2004GL019492, 2004. 150

Rigor, I. G., Colony, R. L., and Martin, S.: Variations in surface air temperature observations in the Arctic, 1979–1997, J. Climate, 13, 896–914, 2000. 148

Rigor, I. G., Wallace, J. M., and Colony, R.: Response of sea ice to the Arctic oscillation, J. Climate, 15, 2648–2663, 2002. 133, 135, 150, 154

Rothrock, D. A. and Wensnahan, M.: The accuracy of sea-ice draft measured from US Navy submarines, J. Atmos. Ocean. Techn., 24, 1936–1949, 2007. 136

Rothrock, D. A. and Zhang, J.: Arctic ocean sea ice volume: what explains its recent depletion?, J. Geophys. Res., 110, C01002, doi:10.1029/2004JC002282, 2005. 133

Rothrock, D. A., Yu, Y., and Maykut, G. A.: Thinning of the Arctic sea-ice cover, Geophys. Res. Lett., 26, 3469–3472, 1999. 136, 144, 145

Shimada, K., Kamoshida, T., Itoh, M., Nishmo, S., Carmack, E., McLaughlin, F., Zimmerman, S., and Proshutinsky, A.: Pacific Ocean inflow: influence on catastrophic reduction of sea ice cover in the Arctic Ocean, Geophys. Res. Lett., 33, L08605, doi:10.1029/2005GL025624, 2006. 148

Steele, M. and Boyd, T.: Retreat of the cold halocline layer in the Arctic Ocean, J. Geophys. Res., 103, 10419–10435, 1998. 148

Thompson, D. W. J. and Wallace, J. M.: The Arctic Oscillation signature in the wintertime geopotential height and temperature fields, Geophys. Res. Lett., 25, 1297–1300, 1998. 133

Thorndike, A. S., Rothrock, D. A., Maykut, G. A., and Colony, R.: The thickness distribution of sea ice, J. Geophys. Res., 80, 4501–4513, 1975. 133

Tucker, W. B., Weatherly, J. W., Eppler, D. T., Farmer, L. D., and Bentley, D. L.: Evidence of rapid thinning of sea ice in the Western Arctic Ocean at the end of the 1980s, Geophys. Res. Lett., 28, 2851–2854, 2001. 144, 145, 146, 147

Vinje, T.: Fram Strait ice fluxes and atmospheric circulaiton: 1950–2000, J. Climate, 14, 3508–3517, 2001. 150

Wadhams, P.: Evidence for thinning of the Arctic ice cover north of Greenland, Nature, 345, 795–797, 1990. 144, 145

Wadhams, P. and Davis, N. R.: Further evidence of ice thinning in the Arctic Ocean, J. Geophys. Res., 27, 3973–3975, 2000. 144, 145

Wadhams, P. and Davis, N. R.: Arctic sea-ice morphological characteristics in summer 1996, Ann. Glaciol., 33, 165–170, 2001. 137, 146

Walsh, J. E. and Chapman, W. L.: Arctic cloud-radiation-temperature associations in observational data and atmospheric reanalysis, J. Climate, 11, 3030–3045, 1998. 153

Walsh, J. E., Chapman, W. L., and Shy, T. L.: Recent decrease of sea level pressure in the central Arctic, J. Climate, 9, 480–486, 1996. 135

Wang, J., Zhang, J., Watanabe, E., Ikeda, M., Mizobata, K., Walsh, J., Bai, X., and Wu, B.: Is the dipole anomaly a major driver to record lows in Arctic summer sea ice extent?, Geophys. Res. Lett., 36, L05706, doi:10.1029/2008GL036706, 2009. 135, 151

Watanabe, E., Wang, J., Zhang, J., Sumi, A., and Hasumi, H.: Arctic dipole anomaly and its conttribution to sea ice export from the Arctic Ocean in the 20th century, Geophys. Res. Lett., 33, L23703, doi:10.1029/2006GL028112, 2006. 133, 151

Wensnahan, M. and Rothrock, D. A.: Sea-ice draft from submarine-based sonar: establishing a consistent record from analog and digitally recorded data, Geophys. Res. Lett., 32, L11502, doi:10.1029/2005GL022507, 2005. 136

Wu, B., Wang, J., and Walsh, J.: Dipole Anomaly in the winter Arctic atmosphere and its association with sea ice motion, J. Climate, 19, 210–225, 2006. 133, 148, 150, 154

Yu, Y., Maykut, G. A., and Rothrock, D. A.: Changes in the thickness distribution of Arctic sea ice between 1958–1970 and 1993–1997, J. Geophys. Res., 109, C08004, doi:10.029/2003JC001982, 2004. 140, 144, 145, 146, 148

Zhang, J., Rothrock, D. A., and Steele, M.: Recent changes in Arctic sea ice: the interplay between ice dynamics and thermodynamics, J. Climate, 13, 3099–3114, 2000. 133, 146, 149, 150, 154

TCD

5, 131–167, 2011

Variability and changes of Arctic sea ice

A. Oikkonen and J. Haapala

Table 1. Number of observations.

Region	Spring 1975–1987	Spring 1988–2000	Autumn 1975–1987	Autumn 1988–2000
1	1 747 984	1 836 011	86 350	1 141 483
2	5 968 831	5 410 771	296 347	6 991 425
3	3 887 367	2 355 295	368 396	4 341 843
4	1 617 896	7 128 444	315 520	7 463 208
5	375 730	5 420 254	346 404	4 682 345
6	4 475 459	8 593 098	305 597	2 933 854

TCD
5, 131–167, 2011

A. Oikkonen and J. Haapala

Table 2. Regional spring and autumn mean and modal draft in 1975–1987 and 1988–2000. The change between periods is listed as absolute difference as well as scaled per decade.

		Mean/modal draft (m)		Change	
Region/	Season	1975–1987	1988–2000	m	m/decade
1	Spring	4.4/2.9	3.6/2.5	−0.8/−0.4	−0.6/−0.3
	Autumn	3.1/2.7	2.8/2.5	−0.3/−0.2	−0.2/−0.2
2	Spring	4.2/2.5	3.4/2.3	−0.8/−0.2	−0.6/−0.2
	Autumn	3.1/2.1	2.4/2.3	−0.7/+0.2	−0.6/+0.2
3	Spring	3.5/2.5	2.5/1.7	−1.0/−0.8	−0.8/−0.6
	Autumn	1.7/1.3	1.5/0.3	−0.2/−1.0	−0.2/−0.8
4	Spring	3.1/2.5	2.4/1.5	−0.7/−1.0	−0.5/−0.8
	Autumn	1.2/0.1	1.4/0.3	+0.2/+0.2	+0.2/+0.2
5	Spring	4.5/2.5	3.1/2.1	−1.4/−0.4	−1.1/−0.3
	Autumn	2.3/1.9	1.9/1.9	−0.4/0	−0.3/0
6	Spring	3.3/0.1	3.4/2.1	+0.1/+2.0	+0.1/+1.5
	Autumn	2.7/1.9	2.8/1.9	+0.1/0	+0.0/0

TCD
5, 131–167, 2011

A. Oikkonen and J. Haapala

Table 3. Difference in total ice volume and in the volume of ice in category 1, 2 and 3 between periods 1975–1987 and 1988–2000.

		Total volume	Category 1	Category 2	Category 3
1	Spring	−18.2%	+17.4%	+27.5%	−46.4%
	Autumn	−9.9%	+8.0%	−9.0%	−12.8%
2	Spring	−16.9%	+68.0%	−3.5%	−35.6%
	Autumn	−24.1%	+1950.3%	−17.6%	−43.5%
3	Spring	−29.3%	+176.4%	−48.8%	−35.7%
	Autumn	−16.8%	+44.9%	−19.5%	−35.4%
4	Spring	−22.6%	+134.3%	−40.1%	−44.1%
	Autumn	+19.0%	−9.8%	+43.6%	−32.8%
5	Spring	−30.9%	+109%	−27.9%	−47.1%
	Autumn	−16.6%	+209.8%	−20.5%	−16.6%
6	Spring	+3.3%	+21.6%	+10.3%	−7.2%
	Autumn	+2.1%	−17.3%	+3.5%	+0.3%

TCD
5, 131–167, 2011

A. Oikkonen and J. Haapala

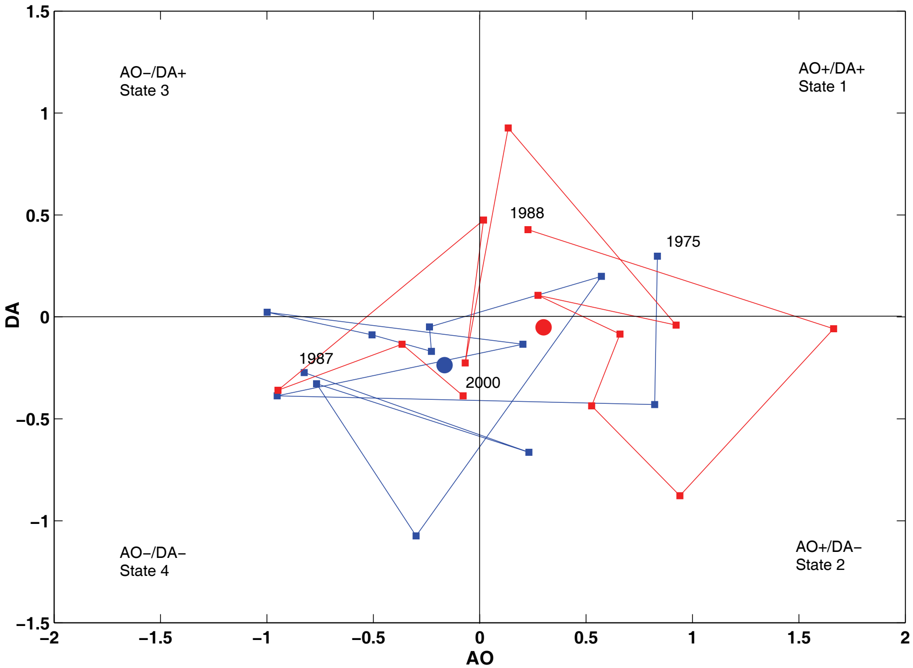

Fig. 1. Annual Artic Oscillation index (AO) and Dipole Anomaly index (DA). Years 1975–1987 are marked with blue and years 1988–2000 with red color. Circles denote the mean values of these 13-year periods.

TCD
5, 131–167, 2011

Variability and changes of Arctic sea ice

A. Oikkonen and J. Haapala

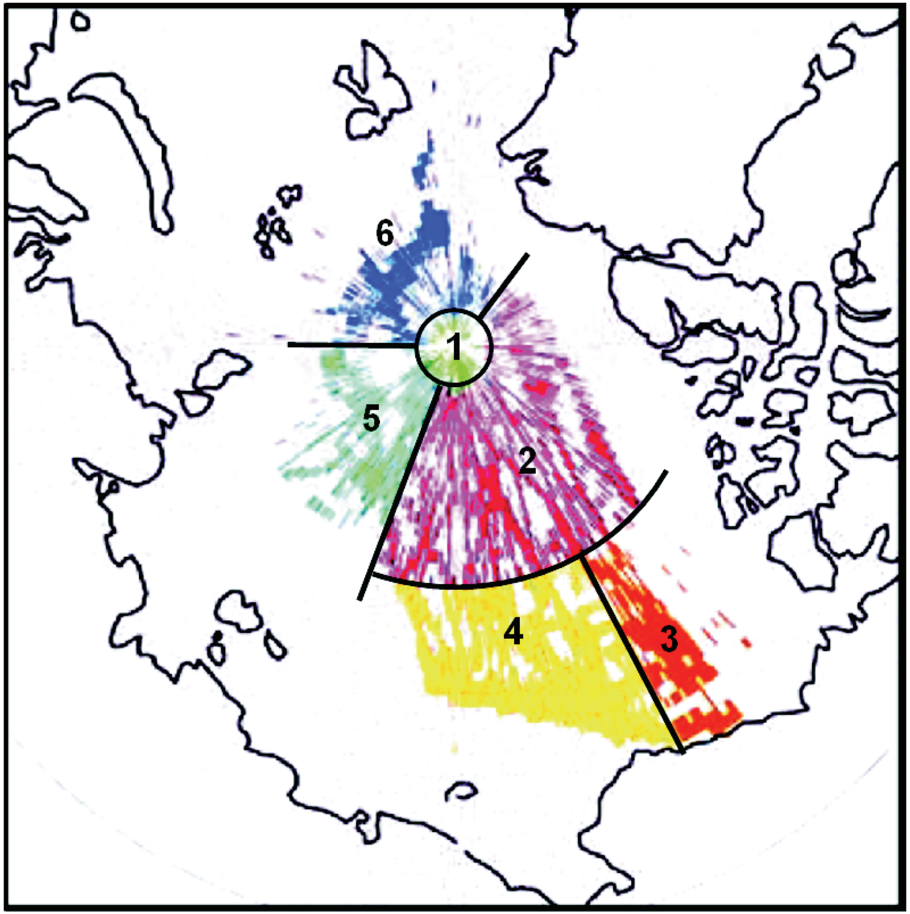

Fig. 2. Area of released data and six regions.

TCD
5, 131–167, 2011

Variability and changes of Arctic sea ice

A. Oikkonen and J. Haapala

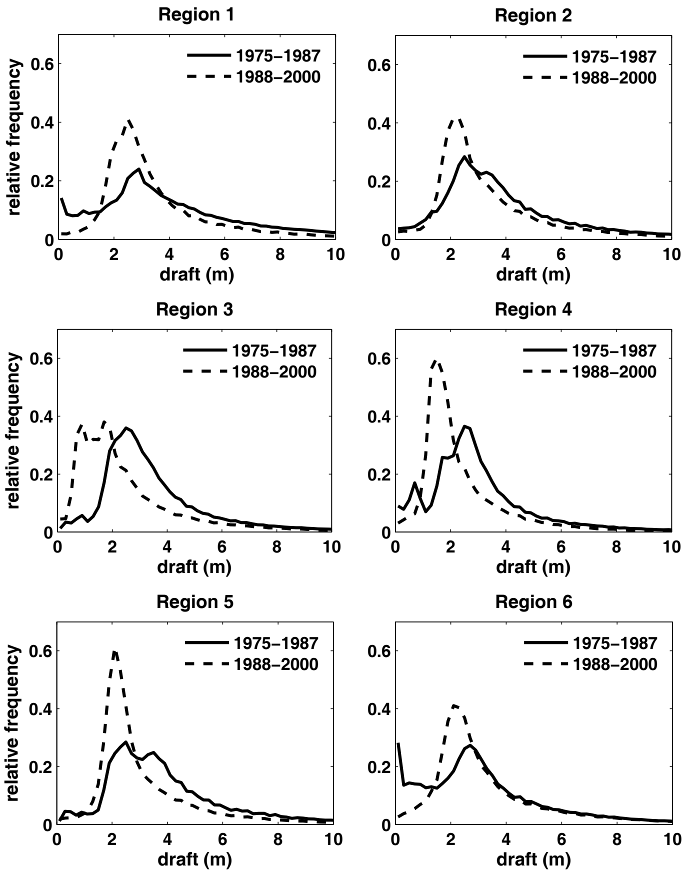

Fig. 3. Regional spring draft distributions during periods 1975–1987 (dashed line) and 1988–2000 (solid line).

TCD
5, 131–167, 2011

A. Oikkonen and J. Haapala

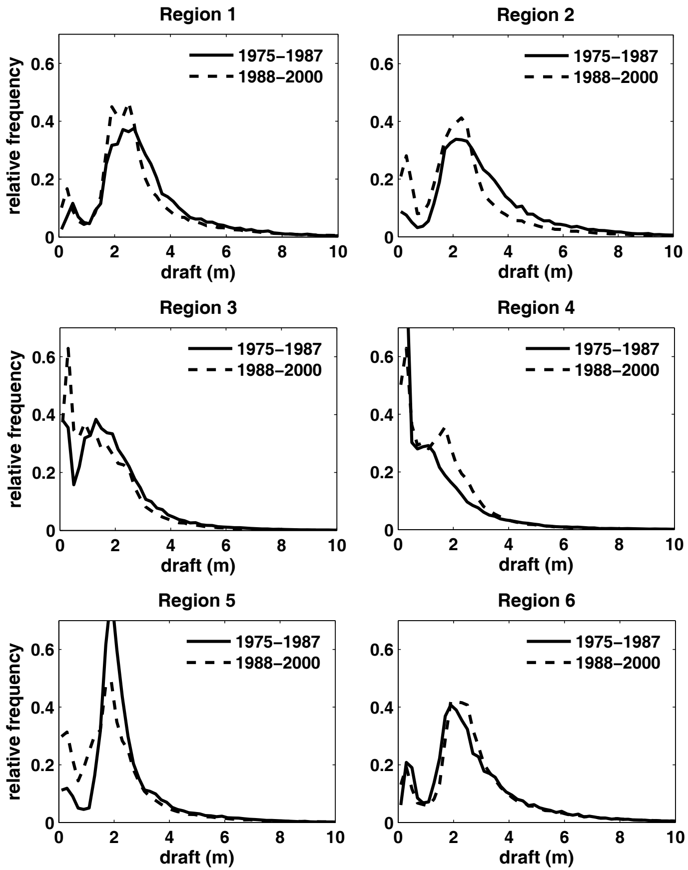

Fig. 4. Regional autumn draft distributions during periods 1975–1987 (dashed line) and 1988–2000 (solid line).

TCD
5, 131–167, 2011

Variability and changes of Arctic sea ice

A. Oikkonen and J. Haapala

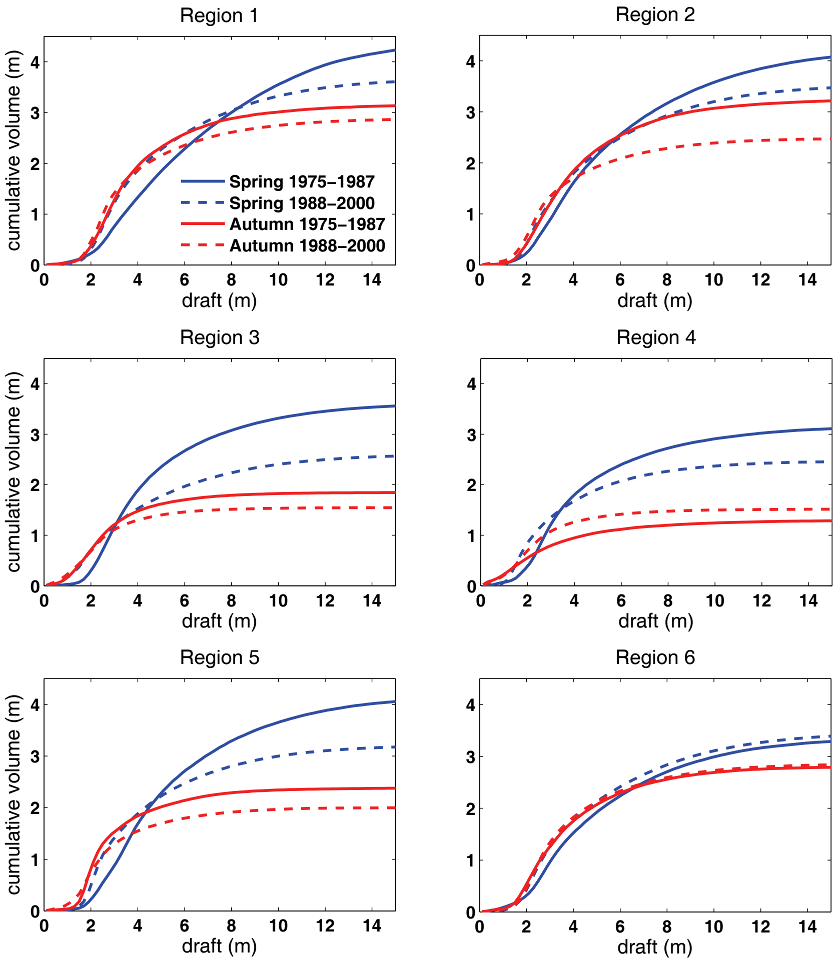

Fig. 5. Regional cumulative ice volume distribution in spring and autumn during the periods 1975–1987 and 1988–2000.

TCD
5, 131–167, 2011

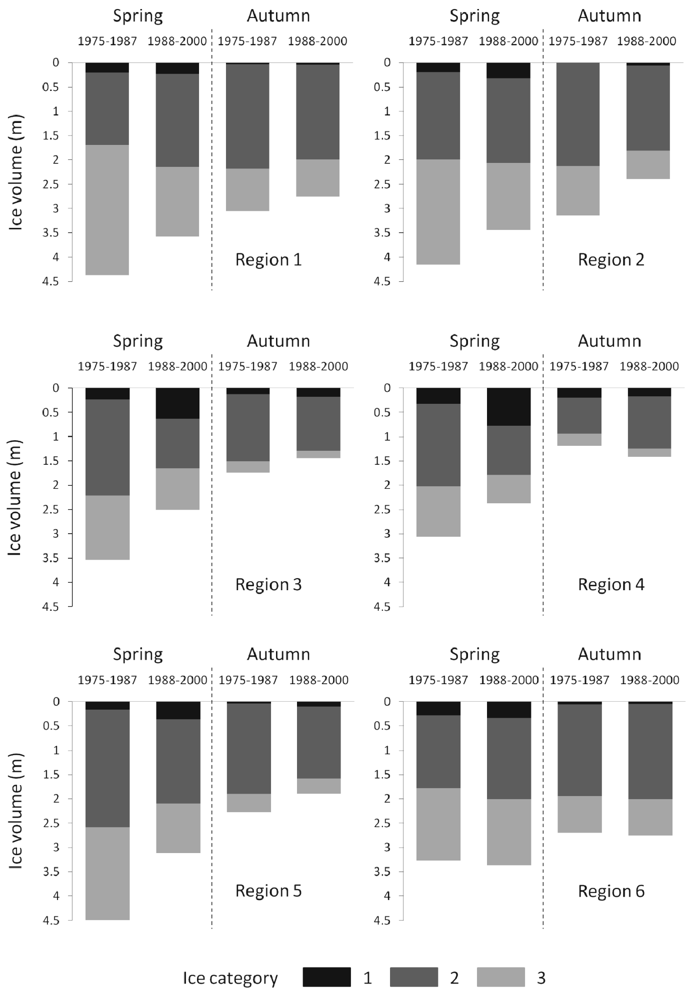

Fig. 6. Regional total ice volume and its composition.

TCD
5, 131–167, 2011

Variability and changes of Arctic sea ice

A. Oikkonen and J. Haapala